ACTA ACUSTICA UNITED WITH ACUSTICA
Vol. 91 (2005) 840 – 845

Inhomogeneous Waves in Piezoelectric Crystals

Nico F. Declercq, Joris Degrieck, Oswald Leroy
Soete Laboratory, Department of Mechanical Construction and Production, Ghent University, Sint Pietersnieuwstraat 41, B-9000 Ghent, Belgium. NicoF.Declercq@Ugent.be

Summary
Inhomogeneous waves are described as pure homogeneous plane waves, except that the wave vector is complex valued. This results in an exponential decay of the amplitude along the wave front. The last 30 years, a lot of studies have been reported on the properties of inhomogeneous waves. It is, for example, known that their velocity depends on the inhomogeneity, in isotropic as well as in anisotropic media. Nevertheless, the influence of piezoelectricity, which is very important for a lot of crystals, has always been neglected in the reported studies. The present paper reports a study of the propagation of inhomogeneous waves in the bulk of piezoelectric crystals. Special attention is drawn on the susceptibility of inhomogeneous waves to the effect of piezoelectricity. Numerical examples are given for Lithium Niobate.

PACS no. 43.20.Bi, 43.20.Hq, 43.35.Cg

1. Introduction

From the very beginning, when inhomogeneous waves made their entry in acoustics, they have been either studied as side effects in scattering problems at interfaces between different media, or as independent physical entities, from a theoretical point of view as well as from an experimental point of view [1]. Most studies have been undertaken for the case of isotropic media. Only a few studies have been reported of inhomogeneous waves in anisotropic media [2, 3, 4, 5, 6, 7, 8, 9, 10, 11].

The present study extends the existing studies to the case where also piezoelectricity is involved. It is known that piezoelectricity results in a change (often called *stiffening effect* [12]) of the elastic constants and this has effects on the propagation of homogeneous plane waves. More precisely, bulk homogeneous waves propagate at different velocities because of this stiffening. In the framework of the study of inhomogenous waves, the question that needs to be resolved is the influence of the piezoelectric effect on inhomogeneous waves. Will this influence be different from the influence on homogeneous plane waves? It will be shown that inhomogeneous waves are more susceptible to the influence of piezoelectricity than homogeneous plane waves. Note that it is well known that inhomogeneous waves also form the building blocks of surface waves, such as Bleustein-Gulyaev waves on piezoelectric crystals [13]. Here however we only consider bulk inhomogeneous waves without any influence of the surface.

Received 27 February 2005,
accepted 6 June 2005.

2. Theoretical development

For piezoelectric materials, taking into account Einstein's double suffix notation convention, the stress tensor [12, 14] is given by

$$\sigma_{ij} = c_{ijkl} e_{kl} - \xi_{kij} E_k, \tag{1}$$

whereas the electrical displacement is given by

$$\boldsymbol{D}_k = \varepsilon_{ki} \boldsymbol{E}_i + \xi_{kij} e_{ij}, \tag{2}$$

where c_{ijkl} is the stiffness tensor, ξ_{kij} is the piezoelectric stress tensor, ε_{ij} is the dielectrical permittivity tensor, $\boldsymbol{E}$ is the electric field vector, $\boldsymbol{D}$ is the dielectric displacement vector and e_{kl} is the strain tensor.

For ultrasonic waves [12], the accompanying electric field is quasistatic and can be described by

$$\boldsymbol{E} = -\nabla \varphi, \tag{3}$$

with φ a scalar potential.

The acoustic wave equation for visco-elastic materials is given by

$$\frac{\partial \sigma_{ij}}{\partial r_j} = \rho \frac{\partial^2 u_i}{\partial t^2}, \tag{4}$$

whereas the electromagnetic field equations, in the absence of electric currents and electric loads are given by

$$\nabla \times \boldsymbol{E} = \mu_0 \frac{\partial \boldsymbol{H}}{\partial t} \tag{5}$$

and

$$\nabla \times \boldsymbol{H} = \frac{\partial \boldsymbol{D}}{\partial t}. \tag{6}$$

Taking into account (3), relations (5)–(6) can be replaced by [12]

$$\nabla \cdot \frac{\partial^2}{\partial t^2}\Big(-\varepsilon_{ki]}\frac{\partial \varphi}{\partial r_i} + \xi_{kij}\frac{\partial u_j}{\partial r_i}\Big) = 0. \tag{7}$$

If we consider plane waves, then, for $\boldsymbol{P}$ being the polarization vector,

$$\boldsymbol{u} = A\boldsymbol{P}\exp\mathrm{i}\big(k_x x + k_y y + k_z z - \omega t\big) \tag{8}$$

and

$$\varphi = B\exp\mathrm{i}\big(k_x x + k_y y + k_z z - \omega t\big). \tag{9}$$

Then, relation (7) immediately involves

$$B = \frac{k_r k_s \xi_{rsq} A P_q}{\varepsilon_{mn} k_m k_n}. \tag{10}$$

Furthermore, combining relations (4) and (7) delivers [12]

$$M_{ip}P_p = 0. \tag{11}$$

Equation (11) is an extension of Christoffel's equation. Only nontrivial solutions $\boldsymbol{P} \neq 0$ are possible whenever

$$\det M = 0. \tag{12}$$

The expression of M_{ij} can be found in [12] and is explicitely given by

$$M_{ip} = k^2\Big(c_{ijpq}t_j t_q + \frac{t_j t_q \xi_{qij} t_m \xi_{mnp} t_n}{t_m \varepsilon_{ms} t_s}\Big) - \rho\omega^2\delta_{ip}, \tag{13}$$

in which the direction is given by its components t_p. Note that in reference [12] the direction t is always real, whereas in this report the direction is generally complex. This is the reason why further on the complex direction will be given by a vector $\boldsymbol{d}$.This 6th degree polynomial (12) is the so called 'stiffened Christoffel's equation'. From [12] we know that the instantaneous Poynting vector is given by

$$F_i\boldsymbol{e}_i = \frac{1}{2}\Big(-\sigma_{ij}\frac{\partial u_j^+}{\partial t} + \varphi\frac{\partial D^+}{\partial t}\Big)\boldsymbol{e}_i, \tag{14}$$

in which the superscript '+' means 'complex conjugate'. Without presuming the wave vector to be real or complex, it can be shown straightforwardly that (14), becomes, for an amplitude equal to unity,

$$F_i = \frac{1}{2}\omega\Big[\big(c_{ilkj}k_k P_l^+ P_j + \big(B(\xi_{kij}k_k - \xi_{ijk}^+ k_k^+)\big)P_j^+ + \varepsilon_{ij}^+ k_j^+ |B|^2\Big]. \tag{15}$$

The average power then corresponds to the real part of $\boldsymbol{F}$, whereas the peak reactive power corresponds to the imaginary part of $\boldsymbol{F}$ [12].

3. Inhomogeneous waves

Inhomogeneous waves can be generated in materials when scattering is involved between lossy media. However, it is also possible to generate inhomogeneous waves by means of a special transducer. Whereas the behavior of inhomogeneous waves in anisotropic media is well described [2, 3, 4, 5, 6, 7, 8, 9, 10, 11], the effect of piezoelectricity has not been considered so far. For piezoelectric materials, only homogeneous plane waves have been studied [12]. A complete historical review of the theory of inhomogeneous waves, can be found in [1]. An inhomogeneous wave is defined as a plane wave having a complex wave vector $\boldsymbol{k}$. The notion of inhomogeneous waves inside the bulk of a piezoelectric crystal, is introduced through the concept of a complex direction. A real direction is then defined as a real vector $\boldsymbol{d}_1$, for which $\boldsymbol{d}_1 \cdot \boldsymbol{d}_1 = 1$. This is generalized to a complex direction $\boldsymbol{d} = \boldsymbol{d}_1 + \mathrm{i}\boldsymbol{d}_2$, for which $\boldsymbol{d}_1 \cdot \boldsymbol{d}_1 = 1$. Then, it is possible to determine the (complex) value l from the following definition:

$$\boldsymbol{k} = l\omega\big(\boldsymbol{d}_1 + \mathrm{i}\boldsymbol{d}_2\big). \tag{16}$$

For every possible complex direction, it is possible to determine l. The number of combinations of $\boldsymbol{d}_1$ and $\boldsymbol{d}_2$ is reduced by introducing a complex direction that, for simplicity, contains no imaginary part along the z-axis. We choose a complex direction for which the real part is directed as would be defined classically, though we add an imaginary part to it in the xy-plane perpendicular to the real part. Then this is normalized in order to make its magnitude equal to unity ($\boldsymbol{d} \cdot \boldsymbol{d}^+ = 1$).

$$\boldsymbol{d}_1 + \mathrm{i}\boldsymbol{d}_2 = \Big[\big(d_{1,x} - \mathrm{i}b\sqrt{1-d_{1,y}^2}\big)\boldsymbol{e}_x + \big(d_{1,y} + \mathrm{i}bd_{1,x}\big)\boldsymbol{e}_y + \big(d_{1,z}\big)\boldsymbol{e}_z\Big] \cdot \Big[\sqrt{1+b^2(2d_{1,x} + d_{1,z}^2)}\Big]^{-1}. \tag{17}$$

In addition, for reasons of simplicity, we also choose a normalized real direction, whence $\boldsymbol{d}_1 \cdot \boldsymbol{d}_1 = 1$. For that reason, given a value of b, we limit the number of possible inhomogeneous waves by reducing the number of degrees of freedom to two, representable by a polar angle and an azimuthal angle of propagation. The parameter b (henceforth called the *inhomogeneity parameter*) is then a measure for the fraction of imaginariness of the complex direction. When the direction (17) is entered in the Christoffel's equation (12), the complex scalar $l = l_1 + \mathrm{i}l_2$ can be resolved. This value then determines the entire complex wave vector $\boldsymbol{k}$ as

$$\boldsymbol{k} = \Big((k_{1,x} + \mathrm{i}k_{2,x})\boldsymbol{e}_x + (k_{1,y} + \mathrm{i}k_{2,y})\boldsymbol{e}_y + (k_{1,z} + \mathrm{i}k_{2,z})\boldsymbol{e}_z\Big)\Big/N, \tag{18}$$

with
$$k_{1,x} = l_1 d_{1,x} + l_2 b\sqrt{1-d_{1,y}^2}, \tag{19}$$

$$k_{2,x} = -l_1 b\sqrt{1-d_{1,y}^2} + l_2 d_{1,x}, \tag{20}$$

$$k_{1,y} = l_1 d_{1,y} - l_2 b d_{1,x}, \tag{21}$$

$$k_{2,y} = l_1 b d_{1,x} + l_2 d_{1,y}, \tag{22}$$
$$k_{1,z} = l_1 d_{1,z}, \tag{23}$$
$$k_{2,z} = l_2 d_{1,z}, \tag{24}$$
$$N = \sqrt{1 + b^2(2d_{1,x}^2 + d_{1,z}^2)}\Big/\omega. \tag{25}$$

4. Numerical results for Lithium Niobate

The physical parameters of Lithium Niobate are given in ref [12] and are summarized as follows:

The density is 4700 kg/m^{-3}.

The elastic constants [$\times 10^{10}$ N/m^2] are

$$C_{33} = 24.5, \quad C_{14} = 0.9, \quad C_{44} = 6.0,$$
$$C_{11} = 20.3, \quad C_{12} = 5.3, \quad C_{13} = 7.5, \tag{26}$$

with

$$C_{15} = C_{16} = C_{25} = C_{26} = C_{35} = C_{36} = C_{45} = C_{46} = C_{34} = 0,$$
$$C_{56} = C_{14}, \quad C_{24} = -C_{14}, \quad C_{55} = C_{44}, \tag{27}$$
$$C_{23} = C_{13}, \quad C_{22} = C_{11}, \quad C_{66} = -C_{12}/2 + C_{11}/2.$$

The piezoelectric constants [C/m^2] are

$$\xi_{31} = 0.2, \quad \xi_{22} = 2.5, \quad \xi_{15} = 3.7, \quad \xi_{33} = 1.3, \tag{28}$$

with

$$\xi_{34} = \xi_{23} = \xi_{25} = \xi_{26} = \xi_{35} = 0,$$
$$\xi_{36} = \xi_{11} = \xi_{12} = \xi_{14} = \xi_{13} = 0, \tag{29}$$
$$\xi_{32} = \xi_{31}; \quad \xi_{16} = -\xi_{22};$$
$$\xi_{21} = -\xi_{22}; \quad \xi_{24} = -\xi_{15}.$$

The dielectric constants [10^{-12} F/m] are

$$\varepsilon_1 = 389, \quad \varepsilon_3 = 257, \tag{30}$$

with

$$\varepsilon_2 = \varepsilon_1, \quad \varepsilon_4 = \varepsilon_5 = \varepsilon_6 = 0. \tag{31}$$

Classically, the (real) wave vector $\boldsymbol{k}$ is replaced by $\boldsymbol{k} = l\omega(d_{1,g}\boldsymbol{e}_g)$ and entered into (12). Then, for each (real) direction $(d_{1,x}, d_{1,y}, d_{1,z})$, the complex eigenvalue l can be determined. This l is then the complex slowness value. In what follows, we will only plot the real part of the slowness value because most often the imaginary part is negligible and it resembles damping along the propagation path, whereas the current paper focuses on the inverse wave velocity of waves. At the same time, the polarization vector $\boldsymbol{P}$ is determined as the eigenvector. Here, for the case of inhomogeneous waves, for each chosen real direction d_1, and a parameter b, the complex value l is determined from (16) and Christoffel's equation (12). We have developed a program that is able to draw 3D slowness surfaces and, when necessary, adds arrows that represent the polarization or the energy flow (the real part of the Poynting vector). The modes are then named after the sound polarization and are labeled as quasi longitudinal (QL), quasi shear horizontal (QSH) and quasi shear vertical (QSV). If it follows that the polarization is mainly directed along the propagation direction, the label QL is added. If the polarization is mainly shear and directed along the XY-plane, the label QSH is added. If the polarization is mainly shear and directed along the Z-axis, the label QSV is added.

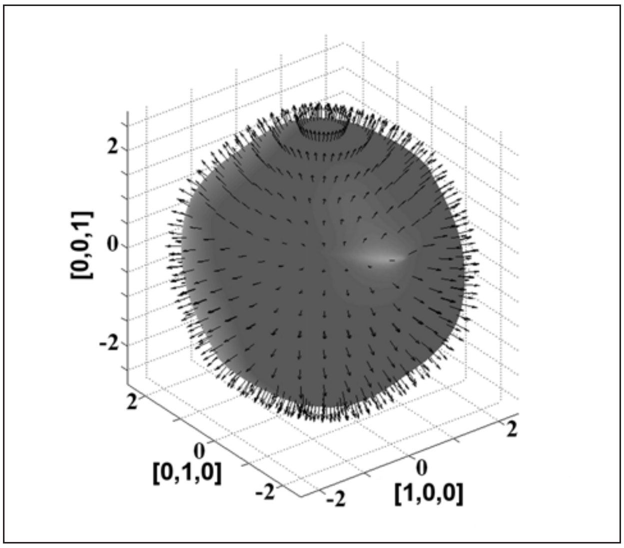

Figure 1. The slowness surface [10^{-4} s/m] for the QSV-mode, in the case of homogeneous plane waves, neglecting piezoelectricity. The associated arrows denote the energy propagation vectors (rescaled for visibility) for each corresponding spot on the slowness surface.

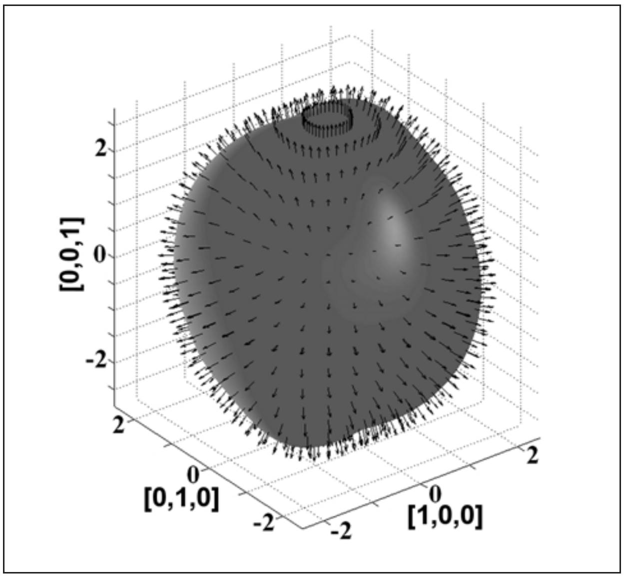

Figure 2. The slowness surface [10^{-4} s/m] for the QSV-mode, in the case of homogeneous plane waves, including piezoelectricity. The associated arrows denote the energy propagation vectors (rescaled for visibility) for each corresponding spot on the slowness surface.

In Figure 1, the slowness surface is depicted for the QSV-mode, in the case of homogeneous plane waves and neglecting piezoelectricity. In addition, arrows are added that correspond to the energy flux direction (the real part

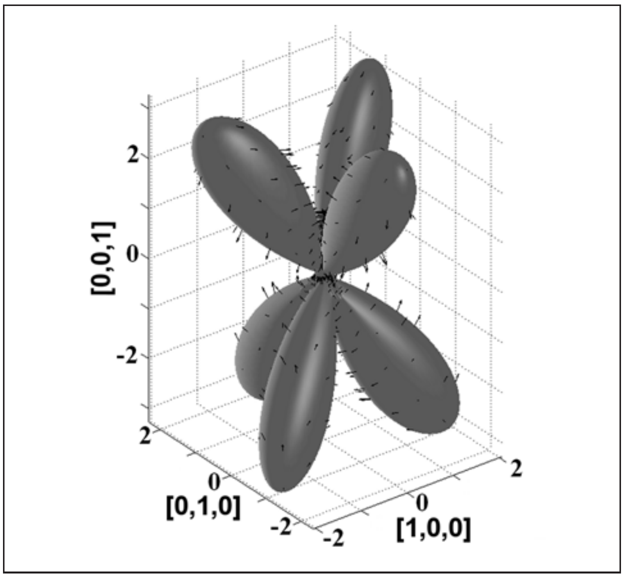

Figure 3. The difference between the case when there is piezoelectricity involved and when the piezoelectric effect is neglected, for the QSV-mode [10^{-5} s/m]. This figure physically corresponds to the difference between Figure 2 and Figure 1, i.e. Figure 2 minus Figure 1. The corresponding arrows denote the difference in energy propagation vector (rescaled for visibility).

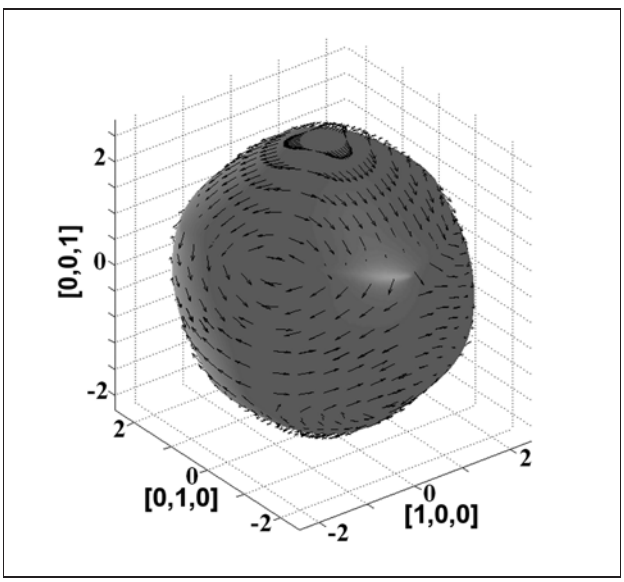

Figure 4. This figure corresponds to Figure 1, except that the arrows here denote the polarization.

of the Poynting vector), rescaled for visibility. If piezoelectricity is considered, a stiffening effect occurs whence the slowness changes, depending on the direction. This is seen in Figure 2, where the slowness curve for the QSV-mode is considered, in the presence of piezoelectricity. Note the difference between Figure 2 and Figure 1. As a matter of fact, it is possible to plot the difference between Figure 2 and Figure 1. This difference, corresponding to the difference between the case of piezoelectricity and the case of non-piezoelectricity, is shown in Figure 3. The arrows correspond to the difference in real Poynting vectors

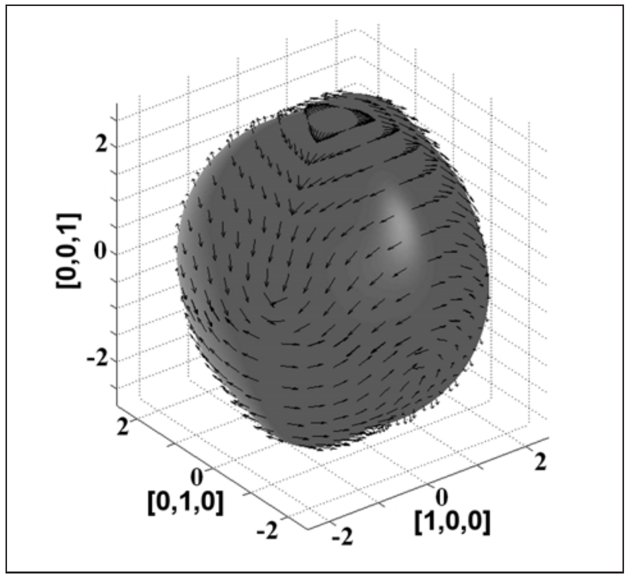

Figure 5. This figure corresponds to Figure 2, except that the arrows here denote the polarization.

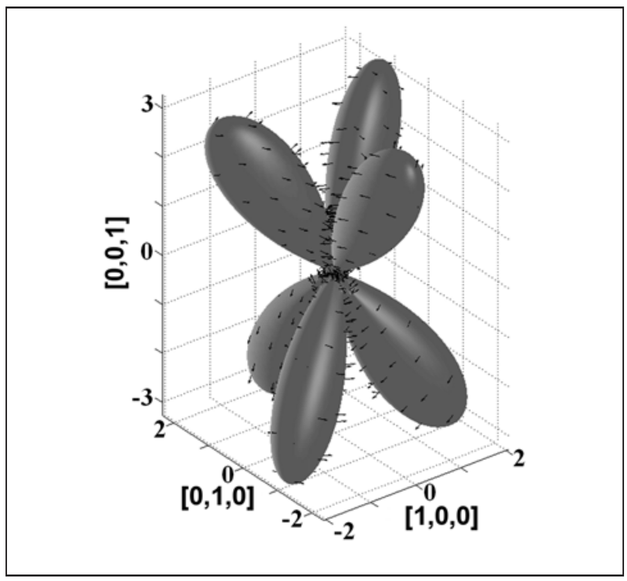

Figure 6. The difference between the case when there is piezoelectricity involved and when the piezoelectric effect is neglected, for the QSV-mode [10^{-5} s/m]. This figure physically corresponds to the difference between Figure 5 and Figure 4. The corresponding arrows denote the difference in polarization (rescaled for visibility). In fact, this figure corresponds to Figure 3, except that the arrows here denote the polarization.

(rescaled for visibility). Note that point-symmetry is preserved in Figure 3 and that some directions do not involve any change of stiffness, whereas others involve changes, resulting in a difference between the slowness. For each considered direction, the difference is plotted.

A similar procedure, for the same QSV-mode, is followed for Figures 4–6, except that now each time, when drawing the arrows, the polarization vectors are considered and not the real Poynting vectors. Note that the piezoelectric effect, besides influencing the energy propagation di-

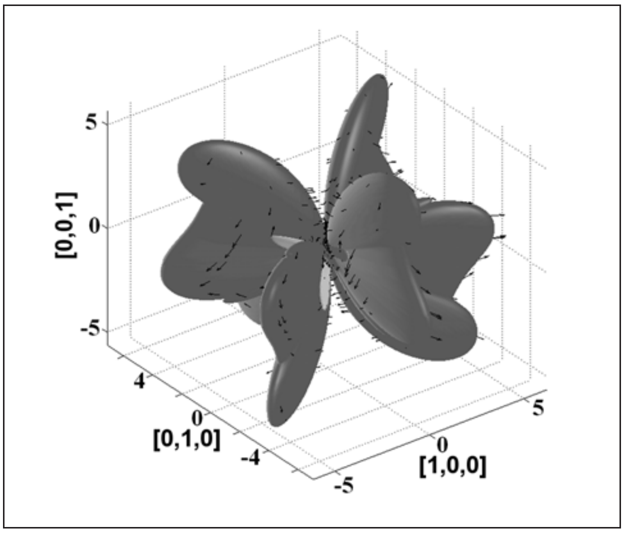

Figure 7. The difference between the case when there is piezoelectricity involved and when the piezoelectric effect is neglected, for the QSV-mode [10^{-5} s/m], in the case of inhomogeneous waves. This figure corresponds to Figure 3, except that inhomogeneous plane waves are considered here, characterized by a parameter of imaginariness $b = 60/140$. The associated arrows denote the difference of the Poynting vector (rescaled for visibility).

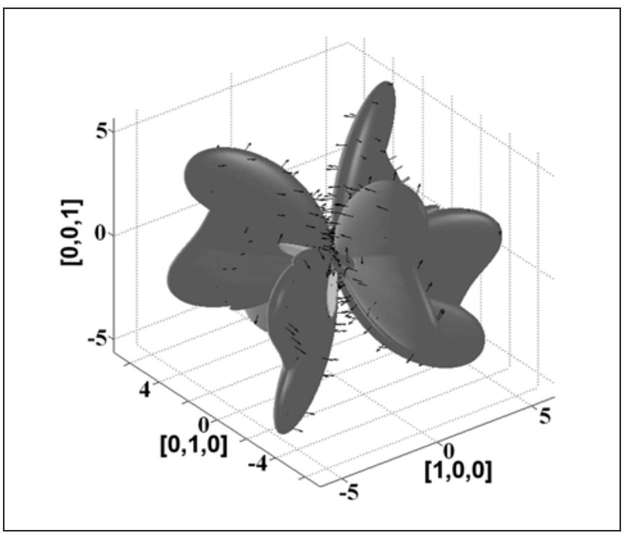

Figure 8. The difference between the case when there is piezoelectricity involved and when the piezoelectric effect is neglected, for the QSV-mode [10^{-5} s/m], in the situation of inhomogeneous waves. The corresponding arrows denote the difference in polarization (rescaled for visibility). As a matter of fact, this figure corresponds to Figure 6, except that inhomogeneous plane waves are considered here, characterized by a parameter of imaginariness $b = 60/140$.

rection, also has a strong influence on the polarization vectors. In what follows, in order to limit the number of presented figures, we only focus on the differences between the case with piezoelectricity and the case without piezoelectricity.

So far, only homogeneous plane waves have been considered, involving a parameter of imaginariness $b = 0$.

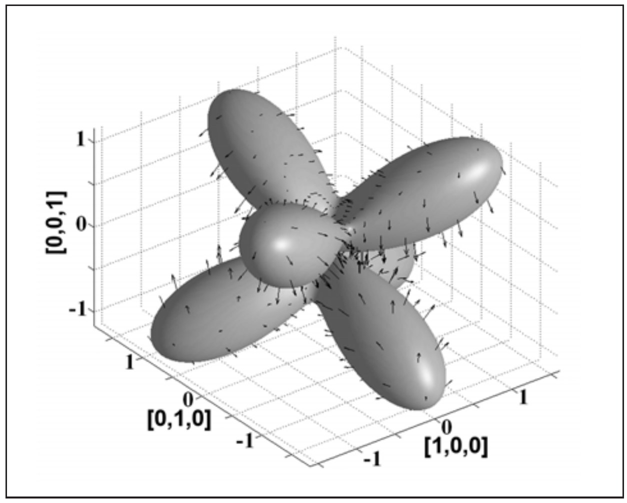

Figure 9. This figure corresponds to Figure 6, i.e. for the case of homogeneous plane waves, except that the QL-mode is considered here.

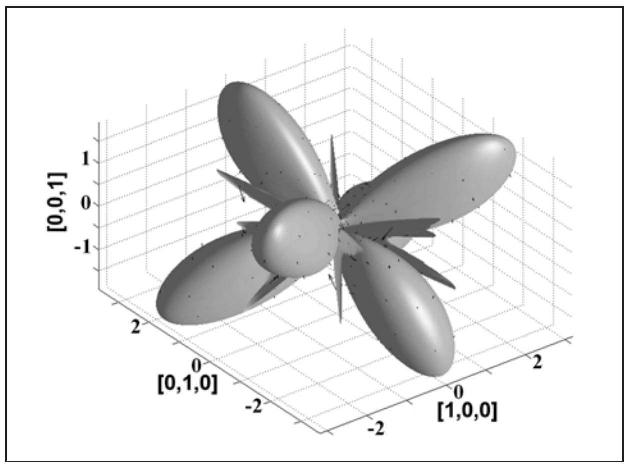

Figure 10. This figure corresponds to Figure 9, except that inhomogeneous plane waves are considered here, characterized by a parameter of imaginariness $b = 60/140$.

Now we consider a parameter $b \neq 0$, resulting in inhomogeneous waves. Figure 7 shows the difference between the slowness surface for the QSV-mode, in the case of $b = 60/140$. The black arrows denote the difference between (the real part of) the Poynting vector for each considered direction.

Comparison between Figure 7 and Figure 3 shows that inhomogeneous waves are more susceptible to piezoelectricity than homogeneous plane waves. The reason is not clear, but it could be a result of the fact that for a considered mode, the presence of an inhomogeneity in the wave front, does not only influence the sound velocity, but also the polarization, whence the considered mode slightly changes its nature and is better influenced by the effect of piezoelectricity.

Figure 8 corresponds to Figure 7, except that, here, the difference of polarization is denoted by the black arrows. Note that indeed the polarization is altered by the presence of the piezo-electric effect.

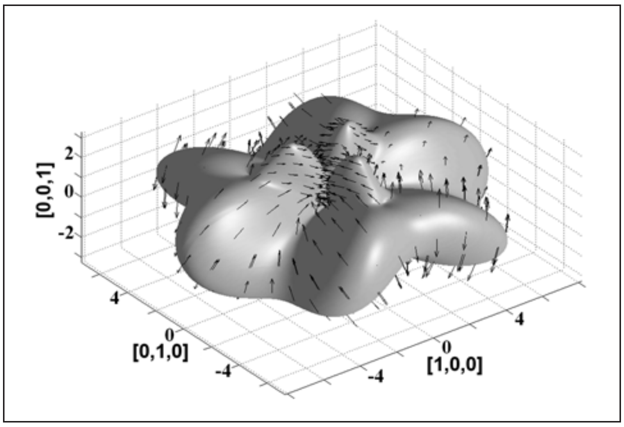

Figure 11. This figure corresponds to Figure 6, i.e. for the case of homogeneous plane waves, except that the QSH-mode is considered here.

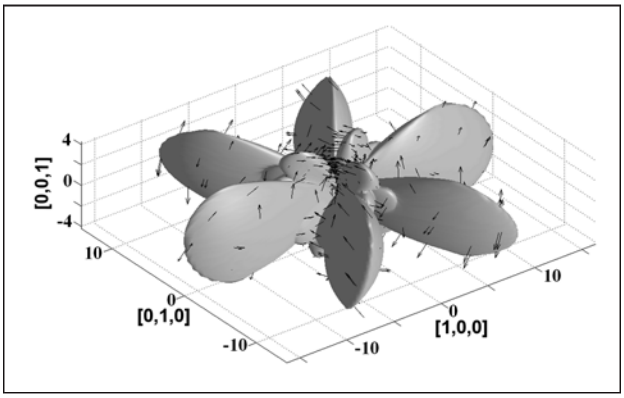

Figure 12. This figure corresponds to Figure 11, except that inhomogeneous plane waves are considered here, characterized by a parameter of imaginariness $b = 60/140$.

In addition, Figure 9 depicts the difference, in slowness surface for homogeneous plane waves, between the case when there is piezoelectricity involved and when the piezoelectric effect is neglected, for the QL-mode. Figure 10 shows that same difference as in Figure 9, except that inhomogeneous plane waves are considered here, characterized by a parameter of imaginariness $b = 60/140$. Figure 11 illustrates the same as Figure 9, except that the QSH mode is considered and Figure 12 demonstrates the same as Figure 10 for the QSH mode.After considering the effect of piezoelectricity on the QL-mode (Figures 9–10) and the QSH-mode (Figures 11–12), it is noticed that also for these modes, the presence of inhomogeneity makes them more susceptible to the piezoelectric effect. Again, the reason is not certain, but it can be due to the change of polarization due to inhomogeneity.

5. Conclusions

The study is valid for any piezoelectric crystal, though it has only been outlined for Lithium Niobate. It is shown that the effect of piezoelectricity is better felt by inhomogeneous plane waves than by homogeneous plane waves. This means that, even though piezoelectric effects are sometimes neglected when studying the interaction of sound with crystals, it is better not to neglect the effect if inhomogeneous waves are generated within the crystal or if the interaction of bounded inhomogeneous [15] waves, with such crystals is considered.

Acknowledgement

Nico F. Declercq is a postdoctoral fellow of the Fund for Scientific Research - Flanders (FWO - Vlaanderen).

References

[1] N. F. Declercq, R. Briers, J. Degrieck, O. Leroy: The history and properties of ultrasonic inhomogeneous waves. IEEE-trans. on UFFC **52** (2005) 776–791.

[2] M. Hayes: Inhomogeneous plane waves. Arch. Ration. Mech. Anal. **85** (1984) 41–79.

[3] S. I. Rokhlin, T. K. Bolland, L. Adler: Reflection and refraction of elastic waves on a plane interface between two generally anisotropic media. J. Acoust. Soc. Am. **79** (1986) 906–918.

[4] B. Hosten, M. Deschamps, B. R. Tittmann: Inhomogeneous wave generation and propagation in lossy anisotropic solids. Application to the characterization of viscoelastic composite materials. J. Acoust. Soc. Am. **82** (1987) 1763–1770.

[5] B. Hosten: Bulk heterogeneous plane waves propagation through viscoelastic plates and stratified media with large values of frequency domain. Ultrasonics **29** (1991) 445–450.

[6] M. Deschamps, B. Hosten: The effects of viscoelasticity on the reflection and transmission of ultrasonic waves by an orthotropic plate. J. Acoust. Soc. Am. **91** (1992) 2007–2015.

[7] P. Lanceleur, H. Ribeiro, J.-F. De Belleval: The use of inhomogeneous waves in the reflection-transmission problem at a plane interface between two anisotropic media. J. Acoust. Soc. Am. **93** (1993) 1882–1892.

[8] M. Deschamps, F. Assouline: Attenuation along the poynting vector direction of inhomogeneous plane waves in absorbing and anisotropic solids. Acustica – Acta Acustica **86** (2000) 295–302.

[9] B. Rogé: Réflexion/transmission d'une onde plane inhomogene incidente sur une interface plane séparant deux milieux anisotropes. Thesis, Université de Technologie de Compiègne, France, 1999.

[10] P. Boulanger, M. Hayes: Special inhomogeneous waves in cubic elastic materials. Zeitschrift fur angewandte Mathematik und Physik **51** (2000) 1031–1038.

[11] M. Deschamps, O. Poncelet: Inhomogeneous plane wave and the most energetic complex ray. Ultrasonics **40** (2002) 293–296.

[12] B. A. Auld: Acoustic fields and waves in solids, Volume I, second edition. Krieger, Florida, 1989.

[13] J. M. Rouvaen, P. Logette, P. Goutin, M. Gazalet, F. Haine: Acousto-optic detection of Bleustein-Gulyaev surface waves propagating on cubic crystals. J. Phys. D: Appl. Phys. **31** (1998) 595–599.

[14] A. H. Nayfeh: Wave propagation in layered anisotropic media. North Holland, Elsevier, 1995.

[15] N. F. Declercq, J. Degrieck, O. Leroy: The Laplace transform to describe bounded inhomogeneous waves. J. Acoust. Soc. Am. **116** (2004) 51–60.